Research Article

Evaluation of the combined activity of benzimidazole arylhydrazones as new anti-Parkinsonian agents: monoamine oxidase-B inhibition, neuroprotection and oxidative stress modulation

https://doi.org/10.4103/1673-5374.309843

Date of submission: June 24, 2020

Date of decision: November 19, 2020

Date of acceptance: January 6, 2021

Date of web publication: March 25, 2021

Neda Anastassova[1, *], Denitsa Aluani[2], Anton Kostadinov[1], Miroslav Rangelov[1], Nadezhda Todorova[3], Nadya Hristova-Avakumova[4], Maria Argirova[1], Nikolay Lumov[1], Magdalena Kondeva-Burdina[2], Virginia Tzankova[2], Denitsa Yancheva[1]

Graphical Abstract *The most promising benzimidazole arylhydrazone 7 as a potential drug for Parkinson's disease with good safety profile and combined MAO-B inhibitive, neuroprotective and antioxidant activity*

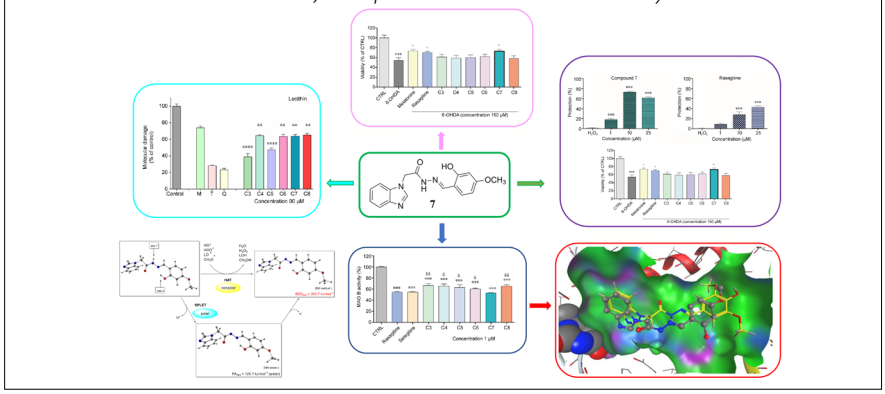

Abstract

Neuroprotective drugs and selective monoamine oxidase inhibitors can slow down the progression and improve symptoms of Parkinson's disease (PD). Since there is an implication of oxidative stress in the pathophysiological mechanisms of the disease, the compounds possessing an ability to reduce the oxidative stress are prime candidates for neuroprotection. Thereby our current study is focused on the development of new multi-target PD drugs capable of inhibiting the activity of monoamine oxidase-B while exerting neuroprotective and antioxidant properties. A small series of benzimidazole derivatives containing hydroxy and methoxy arylhydrazone fragments has been synthesized and the neurotoxicity of the compounds has been evaluated *in vitro* on neuroblastoma SH-SY5Y cells and on isolated rat brain synaptosomes by measuring the cell viability and the levels of reduced glutathione and a good safety profile has been shown. The 2-hydroxy-4-methoxy substituted arylhydrazone 7 was the least toxic on neuronal SH-SY5Y cells and showed the lowest neurotoxicity in rat brain synaptosomes. The neuroprotective properties of the test compounds were further assessed using two models: H_2O_2-induced oxidative stress on SH-SY5Y cells and 6-hydroxydopamine-induced neurotoxicity in rat brain synaptosomes. Compound 7 showed more pronounced neuroprotective activity on SH-SY5Y cells, compared to the referent melatonin and rasagiline. It also preserved the synaptosomal viability and the reduced glutathione levels; the effects were stronger than those of rasagiline and comparable to melatonin. All the tested compounds were capable to inhibit human monoamine oxidase-B enzyme to a significant extent, however, compound 7 exerted the most prominent inhibitory activity, similar to selegiline and rasagiline. The carried out molecular docking studies revealed that the activity is related to the appropriate molecular structure enabling the ligand to enter deeper in the narrow and highly lipophylic active site pocket of the human monoamine oxidase-B and has a favoring interaction with the key amino acid residues Tyr326 and Cys172. Since much scientific evidence points out the implication of iron dyshomeostasis in PD, the compounds were tested to reduce the ferrous iron induced oxidative molecular damage on biologically important molecules in an *in vitro* lecithin containing model system. All the investigated compounds denoted protection effect, stronger than the one of the referent melatonin. In order to support the assignments of the significant neuroprotective and antioxidant pharmacological activities, the radical-scavenging mechanisms of the most promising compound 7 were evaluated using DFT methods. It was found that the most probable free radicals scavenging mechanism in nonpolar phase is the hydrogen atom transfer from the amide group of compound 7, while in polar medium the process is expected to occur by a proton transfer. The current study outlines a perspective leading structure, bearing the potential for a new anti-PD drug. All performed procedures were approved by the Institutional Animal Care Committee of the Medical University of Sofia (Bulgarian Agency for Food Safety with Permission № 190, approved on February 6, 2020).

Key Words: antioxidants; benzimidazoles; density functional theory; hydrazones; monoamine oxidase-B; neurodegenerative disorders; neuroprotection; oxidative stress; Parkinson's disease; synaptosomes

Chinese Library Classification No. R453; R364; R741

[1]Institute of Organic Chemistry with Centre of Phytochemistry, Bulgarian Academy of Sciences, Sofia, Bulgaria; [2]Department of Pharmacology, Pharmacotherapy and Toxicology, Faculty of Pharmacy, Medical University of Sofia, Sofia, Bulgaria; [3]Institute of Biodiversity and Ecosystem Research, Bulgarian Academy of Sciences, Sofia, Bulgaria; [4]Department of Medical Physics and Biophysics, Faculty of Medicine, Medical University of Sofia, Sofia, Bulgaria

*__Correspondence to:__ Neda Anastassova, PhD, Neda.Anastassova@orgchm.bas.bg.

https://orcid.org/0000-0002-2776-0021 (Neda Anastassova)

Funding: *This work was supported by the National Science Fund of Bulgaria (Young scientists project contract КП-06-M29/4; to NA, MA, NHA, and DA).*

How to cite this article: *Anastassova N, Aluani D, Kostadinov A, Rangelov M, Todorova N, Hristova-Avakumova N, Argirova M, Lumov N, Kondeva-Burdina M, Tzankova V, Yancheva D (2021) Evaluation of the combined activity of benzimidazole arylhydrazones as new anti-Parkinsonian agents: monoamine oxidase-B inhibition, neuroprotection and oxidative stress modulation. Neural Regen Res 16(11):2299-2309.*

Introduction

Parkinson's disease (PD) is one of the most prevalent and still incurable neurodegenerative disorders affecting around 10 million people worldwide today. PD results in dopamine (DA) deficiency caused by the progressive death of dopaminergic neurons in the substantia nigra pars compacta, the region of the brain controlling the motor activity by projecting dopaminergic axons to the striatum. Although the traditional levodopa replacement therapy reduces the clinical symptoms for several years after diagnosis by replenishing the levels of striatal DA, it is incapable of preventing the disease progression (Freitas et al., 2016). It has been demonstrated that neuroprotective drugs and selective monoamine oxidase inhibitors, such as selegiline and rasagiline, could slow down the progression and improve symptoms (Wingo et al., 2012). The action of the monoamine oxidase enzymes contributes to the generation of oxidative stress and pathogenesis of neurodegenerative diseases since the process of oxidative deamination of monoamines, including DA, produces H_2O_2 and leads to generating reactive oxygen species (Dezsi and Vecsei, 2017). Because of the tonic activity and dense packing of the dopaminergic neurons, they are particularly vulnerable to oxidative stress. Their degree of oxidative stress increases in early stage of PD since a portion of the neurons is lost and the activity of the remaining ones increases as a compensatory mechanism (Finberg et al., 2016). The inhibition of monoamine oxidase-B (MAO-B) besides prolonging the half-life of DA leading to an extended neurotransmission relieving the motor symptoms, also prevents the further oxidative damages mediated by the enzyme during the DA degradation and decreases the parkinsonian symptoms (Weinreb et al, 2012; Uddin et al., 2020). Having in mind the implication of oxidative stress in the disease pathophysiological mechanisms, the prime candidates for neuroprotection would be compounds possessing the ability to reduce oxidative stress. Despite all the numerous ambitious efforts up to now clinical trials have failed identifying compounds with compelling proof for neuroprotective properties. The search for neuroprotective agents remains among the major challenges for the future PD research.

Up to date, the administration of melatonin has demonstrated a remarkable neuroprotective effect in animal models of PD, and has shown promising results in improving the motor deficits. The drug rasagiline has a potent MAO-B inhibitory activity and also exhibits neuroprotective activity *in vitro* and *in vivo* by increasing the survival of cultured fetal mesencephalic dopaminergic neurons (Inaba-Hasegawa et al., 2017) and has a neuroprotective effect in dopaminergic neuroblastoma cells (Wu et al., 2017). However, rasagiline has been related to adverse side effects such as dizziness, headache, hallucinations, restlessness, muscular soreness, fatigue, pain, nausea and xerostomia, elevated liver enzymes, abdominal pain, as well as cases of melanoma (Hattori et al., 2019). Recently broad series of oxindole based compounds have been synthesized using rasagiline as a leading compound with indicative neuroprotective properties capable of preventing neuronal cell death through attenuation of oxidative stress. The compounds contain various benzaldehyde structural motifs (Hirata et al., 2018). The presence of an amino or imino group has an essential role in the orientation and complex formation at the active site of the enzyme, examples of which are iproniazid and isocarboxazid, used in the past bearing hydrazone moieties. Moreover, in other studies substituted hydrazides and hydrazones have been reported as MAO inhibitors (Carradori et al., 2015, 2018; Carradori and Silvestri, 2015; Secci et al., 2019).

Our previous studies on 1,3-disubstituted benzimidazole derivatives containing arylhydrazone functionalities and residues of vanillin and syringaldehyde conducted on isolated synaptosomes demonstrated low neurotoxicity in combination with enhanced neuroprotective and antioxidant effects, identical to melatonin and thereby a promising potential for the development of new pharmaceuticals for the treatment of neurodegenerative disorders (Anastassova et al., 2019, 2020). Encouraged by these results, we are currently presenting a small series of N-monoalkylated benzimidazole based MAO-B inhibitors exhibiting combined neuroprotective and antioxidant action with potential application for the treatment of PD.

Materials and Methods

Materials

The chemicals and reagents employed in the synthesis of compounds 1–8 were purchased from Sigma-Aldrich (Merck KGaA, Darmstadt, Germany) and Alfa Aesar (Thermo Fisher GmbH, Kandel, Germany). The progress of the reaction and purity of the products were checked by thin layer chromatography on standard silica gel pre-coated plates (60 F254, 0.25 mm, Merck KGaA, Darmstadt, Germany). The column chromatography was performed using silica gel (Merck Silica gel 60, 0.2–0.5 mm; 35–70 mesh American Standard Test Method).

Melting point measurements

The melting points (MP) of the solid products were measured by Büchi B-540 instrument (Büchi Labortechnik AG, Flawil, Switzerland).

Infrared spectroscopy

All FTIR spectra were recorded on a Bruker Tensor 27 FT spectrometer (Bruker Optics, Ettlingen, Germany) in attenuated total reflectance (ATR) mode, by 64 scans at 2 cm^{-1} resolution.

Nuclear magnetic resonance spectroscopy

Nuclear magnetic resonance (NMR) spectra were measured on a Bruker Avance II+ 600 MHz NMR spectrometer (Bruker Optics, Ettlingen, Germany) using the solvent signal as a reference.

Synthesis

Synthesis of ethyl 2-(1H-benzo[d]imidazol-1-yl)acetate 1

A solution of 1H-benzimidazole (0.0085 mol) in dry dimethylformamide (100 mL) was stirred for 30 minutes with anhydrous potassium carbonate (0.0085 mol). Then tetrabutylammonium hydrogen sulfate (0.0002 mol) was added. After cooling the mixture using an ice bath, 0.0093 mol of ethyl bromoacetate were added slowly dropwise. The mixture was stirred vigorously at room temperature for 8–10 hours and monitored by thin-layer chromatography - (ethyl acetate/n-hexane = 4:1). After the reaction completion, the solid was filtered off and the organic solvent was removed under reduced pressure. The obtained ester was purified by column chromatography using ethyl acetate/n-hexane = 4:1 as eluent.

2-(1H-benzimidazol-1-yl)acetate (1): yield 60%; MP 145–146°C, white solid, purified by column chromatography, eluent ethyl acetate/n-hexane = 4:1; IR (ATR) (ν_{max}/cm^{-1}): 3059, 3025 ($\nu_{C\text{-}H\ Ar}$), 2921, 2848 ($\nu_{C\text{-}H\ Alk}$), 1743 ($\nu_{C=O}$), 1452 ($\gamma_{C\text{-}H\ Ar}$), 1179 ($\nu_{C\text{-}O}$); ^{1}H NMR (600 MHz, DMSO-d_6) δ(ppm): 8.19 (s, 1H, CH), 7.65–7.67 (d, *J* = 7.8 Hz, 1H, Ar-H), 7.52–7.54 (d, *J* = 7.7 Hz, 1H, Ar-H), 7.20–7.26 (m, 2H, Ar-H), 5.25 (s, 2H, CH_2), 4.15–4.18 (m, 2H, CH_2), 1.20–1.23 (t, *J* = 14.6, 7.7 Hz, 3H, CH_3).

Synthesis of 2-(1H-benzo[d]imidazol-1-yl)acetohydrazide 2

To a solution of the benzimidazole ester derivative 1 (0.0045 mol) in 10 mL ethanol was added hydrazine hydrate (0.0090 mol) and the mixture was refluxed for 1 hour. The reaction was monitored using thin-layer chromatography (benzene/methanol = 4:1). After completion of the reaction, the mixture

was cooled down and the formed white crystal mass was filtered off.

2-(1H-benzimidazol-1-yl)acetohydrazide (2): yield 81%; MP 119–120°C, white crystals, purified by column chromatography, eluent ethanol; IR (ATR) (ν_{max}/cm^{-1}): 3285 (ν_{NH2}), 3191 (ν_{NH}), 1654, 1675 ($\nu_{C=O}$), 1616 (δ_{NH2}), 1529 (δ_{NH}); ^{1}H NMR (600 MHz, DMSO-d$_6$) δ(ppm): 9.53 (s, 1H, NH), 8.17 (s, 1H, CH), 7.64–7.65 (m, 1H, Ar-H), 7.46–7.48 (d, 1H, *J* = 7.9 Hz, Ar-H), 7.23–7.26 (m, 1H, Ar-H), 7.19–7.21 (m, 1H, Ar-H), 4.90 (s, 2H, CH_2), 4.36 (s, 2H, NH_2).

General procedure for preparation of compounds 3–8

To a solution of the hydrazide derivative 2 (1.0 equiv) in absolute ethanol were added the respective hydroxy and methoxy benzaldehydes (1.0 equiv). The reaction was refluxed for 1–6 hours. The progress of the reaction was monitored using thin-layer chromatography (benzene/methanol = 4:1). The precipitated product was filtered and washed with ethanol.

2-(1H-benzo[d]imidazol-1-yl)-N′-(2,3-dihydroxybenzylidene) acetohydrazide (3): yield 60%; MP 214–215°C, white crystals, recrystallized from ethanol; IR (ATR) (ν_{max}/cm^{-1}): 3451 (ν_{OH}), 3101 (ν_{NH}), 1684 ($\nu_{C=O}$), 1513 (δ_{NH}), 1270 (ν_{C-N}), 1210 (ν_{C-O}); ^{1}H NMR (600 MHz, DMSO-d$_6$) δ (ppm): 11.62 (s, 1H, NH, exchangeable with D_2O), 8.36 (s, 1H, CH), 8.20 (s, 1H, CH), 7.65–7.68 (m, 1H, Ar-H), 7.53–7.56 (d, *J* = 6.7 Hz, 1H, Ar-H), 7.19–7.27 (m, 3H, Ar-H), 6.82–6.89 (m, 1H, Ar-H), 6.69–6.73 (m, 1H, Ar-H), 5.53 (s, 2H, CH_2); ^{13}C NMR (150 MHz, DMSO-d$_6$) δ(ppm): 168.59, 163.71, 148.77, 146.41, 146.04, 145.77, 145.45, 142.56, 135.22, 122.70, 121.80, 121.06, 119.89, 117.18, 111.10, 45.82.

2-(1H-benzo[d]imidazol-1-yl)-N′-(2,4-dihydroxybenzylidene) acetohydrazide (4): yield 78%; MP 249–251°C, white crystals, recrystallized from ethanol; IR (ATR) (ν_{max}/cm^{-1}): 3216 (ν_{OH}), 3105 (ν_{NH}), 1671 ($\nu_{C=O}$), 1517 (δ_{NH}), 1240 (ν_{C-N}), 1202 (ν_{C-O}); ^{1}H NMR (600 MHz, DMSO-d$_6$) δ (ppm): 11.50 (s, 1H, OH, exchangeable with D_2O), 11.06 (s, 1H, OH, exchangeable with D_2O), 10.05 (s, 1H, NH, exchangeable with D_2O), 8.35 (s, 1H, CH), 8.24 (s, 1H, CH), 7.66 (m, 1H, Ar-H), 7.58–7.60 (d, *J* = 8.9 Hz, 1H, Ar-H), 7.50–7.54 (m, 1H, Ar-H), 7.26–7.28 (m, 1H, Ar-H), 7.20–7.23 (m, 2H, Ar-H), 6.34 (s, 1H, Ar-H), 6.28–6.30 (d, *J* = 2.3 Hz, 1H, Ar-H), 5.49 (s, 2H, CH_2); ^{13}C NMR (150 MHz, DMSO-d$_6$) δ(ppm): 167.90, 158.55, 158.30, 152.18, 149.16, 141.63, 116.66, 112.94, 102.15, 96.07, 93.62, 71.27, 61.48, 56.51, 48.91.

2-(1H-benzo[d]imidazol-1-yl)-N′-(3,4-dihydroxybenzylidene) acetohydrazide (5): yield 67%; MP 286–287°C, white crystals, recrystallized from ethanol; IR (ATR) (ν_{max}/cm^{-1}): 3464 (ν_{OH}), 3179, 3097 (ν_{NH}), 1672 ($\nu_{C=O}$), 1511 (δ_{NH}), 1283 (ν_{C-N}), 1224 (ν_{C-O}); ^{1}H NMR (600 MHz, DMSO-d$_6$) δ (ppm): 11.62 (s, 1H, NH, exchangeable with D_2O), 9.45 (s, 2H, OH, exchangeable with D_2O), 8.21 (s, 1H, CH), 7.88 (s, 1H, CH), 7.64–7.66 (d, *J* = 7.2 Hz, 1H, Ar-H), 7.51–7.52 (d, *J* = 7.2 Hz, 1H, Ar-H), 7.19–7.23 (m, 3H, Ar-H), 6.96–6.97 (m, 1H, Ar-H), 6.78–6.79 (m, 1H, Ar-H), 5.50 (s, 2H, CH_2); ^{13}C NMR (150 MHz, DMSO-d$_6$) δ(ppm): 168.46, 163.35, 148.63, 148.53, 148.41, 146.21, 146.19, 145.66, 145.27, 135.22, 125.87, 125.82, 122.92, 122.75, 122.08, 121.84, 121.31, 120.77, 119.86, 119.70, 116.06, 116.00, 113.31, 113.04, 111.06, 110.82, 46.47, 45.81, 31.18.

2-(1H-benzo[d]imidazol-1-yl)-N′-(4-hydroxy-3-methoxybenzylidene)acetohydrazide) (6): yield 70%; MP 267–268°C, white crystals, recrystallized from ethanol; IR (ATR) (ν_{max}/cm^{-1}): 3483 (ν_{OH}), 3194, 3102 (ν_{NH}), 1682 ($\nu_{C=O}$), 1513 (δ_{NH}), 1265 (ν_{C-N}), 1199 (ν_{C-O}); ^{1}H NMR (600 MHz, DMSO-d$_6$) δ(ppm): 11.61 (s, 1H, NH), 9.65 (s, 1H, OH, exchangeable with D_2O), 8.22 (s, 1H, CH), 7.94 (s, 1H, CH), 7.64–7.66 (m, 1H, Ar-H), 7.52–7.53 (m, 1H, Ar-H), 7.35–7.36 (d, *J* = 1.9 Hz, 1H Ar-H), 7.19–7.25 (m, 2H, Ar-H), 7.13–7.14 (m, 1H Ar-H), 6.82–6.84 (d, *J* = 8.2, 1H, Ar-H), 5.54 (s, 2H, CH_2), 3.83 (s, 3H, CH_3); ^{13}C NMR (150 MHz, DMSO-d$_6$) δ(ppm): 168.62, 149.37, 148.47, 145.66, 145.02, 143.64, 125.86, 122.89, 122.73, 122.63, 122.05, 121.83, 119.71, 115.97, 111.06, 109.95, 56.08, 55.99, 45.94, 31.18.

2-(1H-benzo[d]imidazol-1-yl)-N′-(2-hydroxy-4-methoxybenzylidene)acetohydrazide) (7): yield 78%; MP 246–247°C, white crystals, recrystallized from ethanol; IR (ATR) (ν_{max}/cm^{-1}): 3150 (ν_{OH}), 3105 (ν_{NH}), 1686 ($\nu_{C=O}$), 1511 (δ_{NH}), 1259 (ν_{C-N}), 1200 (ν_{C-O}); ^{1}H NMR (600 MHz, DMSO-d$_6$) δ(ppm): 11.58 (s, 1H, OH, exchangeable with D_2O), 10.25 (s, 1H, NH, exchangeable with D_2O), 8.38 (s, 1H, CH), 8.21–8.23 (d, *J* = 16.1 Hz, 1H, CH), 7.65–7.72 (m, 2H, Ar-H), 7.45–7.54 (m, 1H, Ar-H), 7.19–7.28 (m, 2H, Ar-H), 6.50–6.52 (d, *J* = 9.1 Hz, 1H Ar-H), 6.46 (s, 1H, Ar-H), 5.52 (s, 2H, CH_2), 3.75 (s, 3H, CH_3); ^{13}C NMR (150 MHz, DMSO-d$_6$) δ(ppm): 168.30, 162.67, 159.64, 158.42, 148.62, 145.10, 142.44, 131.23, 128.39, 122.74, 119.65, 113.47, 110.82, 106.90, 101.54, 55.66, 45.82.

2-(1H-benzo[d]imidazol-1-yl)-N′-(4-hydroxy-3,5-dimethoxybenzylidene)acetohydrazide) (8): yield 62%; MP 246–251°C (decomposition), white crystals, recrystallized from ethanol; IR (ATR) (ν_{max}/cm^{-1}): 3207 (ν_{OH}), 3109 (ν_{NH}), 1683 ($\nu_{C=O}$), 1512 (δ_{NH}), 1267 (ν_{C-N}), 1213 (ν_{C-O}); ^{1}H NMR (600 MHz, DMSO-d$_6$) δ(ppm): 11.62 (s, 1H, NH, exchangeable with D_2O), 8.23 (s, 1H, CH), 7.90 (s, 1H, CH), 7.65–7.68 (m, 1H, Ar-H), 7.52-7.54 (m, 1H, Ar-H), 7.19–7.27 (m, 2H, Ar-H), 6.82–6.69 (m, 2H, Ar-H), 5.53 (s, 2H, CH_2), 3,81 (m, 6H, CH_3); ^{13}C NMR (150 MHz, DMSO-d$_6$) δ(ppm): 168.30, 162.67, 159.64, 158.42, 148.70, 145.65, 143.63, 135.17, 122.70, 121.80, 119.70, 111.05, 104.99, 56.40, 46.56.

Cell culture and cultivation

The SH-SY5Y neuroblastoma cell line was obtained from the European Collection of Cell Cultures (ECACC, Salisbury, UK). The cells were cultured with 10% complete medium (RPMI 1640 medium, 10% heat inactivated fetal bovine serum, L-glutamine (2 mM)), in 75 cm^2 flasks, in a humidified, 5% CO_2, 37°C incubator (Esco, CCl-170B-8, Elta 90, Singapure).

***In vitro* cell viability assay**

Cell viability was determined by a mitochondria enzyme-dependent reaction of methylthiazolyldiphenyl-tetrazolium bromide (MTT; Sigma-Aldrich Chemie GmbH, Schnelldorf, Germany). Briefly SH-SY5Y cells were seeded in 96-well microplates at a density 2.5 × 10^4 cells/well and allowed to attach to the well surface at 37°C in a humidified atmosphere with 5% CO_2 (24 hours). Nine different concentrations of compounds (1, 10, 25, 50, 75, 100, 250, 500 and 1000 μM) were added to cells, and incubated for 24 hours. For each concentration a set of at least 8 wells were used. After 24 hours of treatment the solution in each well was substituted with MTT solution (0.5 mg/mL in culture medium). The microplates were further incubated for 3 hours at 37°C and the obtained formazan crystals were dissolved by 100 μL/well of DMSO. The absorbance was measured in a multiplate reader Synergy 2 (BioTek Instruments, Inc, Highland Park, Winooski, USA) at 570 nm (690 nm for background absorbance) (Mosmann et al., 1983).

***In vitro* model of H_2O_2-induced oxidative stress**

The possible antioxidant effects of the new arylhydrazone benzimidazole derivatives were evaluated *in vitro* in a model of H_2O_2-induced oxidative stress. SH-SY5Y cells were seeded at a density of 3.5 × 10^4/well in 96-well plates and allowed to attach at the wells bottom for 24 hours. Thereafter the cell medium was aspirated and the cells were treated with solutions of the test compounds (final concentrations: 1, 10, and 25 μM) in RPMI for 60 minutes before H_2O_2 exposure. Afterwards the SH-SY5Y cells were washed with phosphate-buffered saline (PBS) to remove the extracellular amount of the test compounds. Subsequently the treatment with a solution of hydrogen

peroxide (H_2O_2, 1 mM) in PBS for 15 minutes accomplished the SH-SY5Y damage. Rasagiline and melatonin (Sigma-Aldrich Chemie GmbH) were used as reference compounds because of their well-established protective activity (Watson et al., 2016; Matos et al., 2020). In this model, two controls were used: positive control – cells treated with H_2O_2, 1 mM in PBS and negative control – cells, treated with PBS. The contents of all wells were changed with fresh medium and incubated. All procedures related to washing with PBS, change of the cell medium and treatment of the cells with the solutions of the test compounds or hydrogen peroxide were performed by precision aspiration of the liquid above the cells. After 24 hours, the amount of attached viable cells was evaluated by MTT assay. Negative controls (cells without hydrogen peroxide treatment) were considered as 100% protection and hydrogen peroxide-treated cells as 0% protection.

Measurement of MAO-B enzymatic activity

The inhibitory effects of the test compounds on human recombinant MAO-B (hMAO-B) enzyme were studied by the Amplex UltraRed reagent (Sigma-Aldrich Chemie GmbH) fluorometric method (Bautista-Aguilera et al. (2014). Tyramine hydrochloride was used as a substrate. The working solutions of the compounds, reagents and hMAO-B as well as the reaction buffers were prepared according to the producer's instructions. The reaction mixture contained a stock solution of Amplex Red (10 mM) in dimethyl sulfoxide (DMSO), the reaction buffer (0.05 M sodium phosphate) at pH 7.4 and the storage solution of horseradish peroxidase (10 U/mL). As controls were used pure MAO-B working solutions in reaction buffer and MAO-B working solution containing hydrogen peroxide. The final concentration of the compounds in the well was 1 μM. The compounds together with hMAO-B were embedded in a 96-well plate (8 wells for each compound), and then the plate was incubated for 30 minutes (dark, at 37°C). After this incubation time, the reaction was initiated by 50 μL Mix Solution: Amplex®Red reagent, horseradish peroxidase, and tyramine, as an enzyme substrate, in the reaction buffer. The fluorescence was measured every 30 minutes at 0, 30, 60, 90, 120 and 150 minutes), in dark, while shaking the reaction mixture at constant temperature of 37°C. The fluorimetric measurements were assessed using a Synergy 2 Microplate Reader at two wavelengths (570 nm and 690 nm).

Animals

Fifteen male Wistar rats with body weight 200–250 g were used. They were purchased from the National Breeding Center, Sofia, Bulgaria. Food and water were provided ad libitum. Seven days of acclimatization were allowed before the study. The rats were anesthetized with ether by inhalation and perfused through the left ventricle with Tris-buffered saline, prior to decapitation. The brains were quickly removed immediately after decapitation, rinsed with the perfusion buffer and used for the preparation of synaptosomes and microsomes. All further operations were carried out at 4°C. The animal's health was regularly monitored by a veterinary physician. All performed procedures were approved by Institutional Animal Care Committee of Medical University of Sofia (Bulgarian Agency for Food Safety with Permission № 190, approved on February 6, 2020) and were carried out according to Ordinance No. 15/2006 for humane treatment of experimental animals (vivarium certificate of registration of farm No. 0072/01.08.2007).

Isolation and incubation of synaptosomes

The synaptosomes were isolated from the brains of adult male Wistar rats described by Taupin et al. (1994). The brains were homogenized in cold buffer 1 (5 mM HEPES and 0.32 M sucrose (pH 7.4)). Thereafter the homogenate was centrifuged twice and the supernatant was collected and centrifuged 3 times at 4°C. The pellet was re-suspended in ice-cold buffer 1. The rat brain synaptosomes were isolated using Percoll reagent to prepare the gradient. Synaptosomes were re-suspended and incubated in buffer 2 (290 mM NaCl, 0.95 mM $MgCl_2x6H_2O$, 10 mM KCl, 2.4 mM $CaCl_2xH_2O$, 2.1 mM NaH_2PO_4, 44 mM HEPES, 13 mM D-glucose). The incubation of synaptosomes was performed in a 5% CO_2 + 95% O_2 atmosphere. The content of synaptosomal protein was determined according to the method of Lowry et al. (1951) using bovine serum albumin as a standard.

Synaptosomal viability and glutathione assay

Rat brain synaptosomes are a useful system for studying neuronal metabolism and toxicity. They constitute the subcellular fraction prepared from brain tissue and contain synaptic vesicles (as a source for neurotransmitters), synaptic plasma membranes, and synaptic junctional complexes (Jhou et al., 2017). The evaluation of the potential neurotoxic effects of the arylhydrazone benzimidazole derivatives was performed on freshly isolated rat brain synaptosomes. Synaptosomal viability was determined by using MTT-test after treatment with compounds 3, 4, 5, 6, 7 and 8 (50, 100, and 200 μM) (Mungarro-Menchaca et al., 2002). Synaptosomes were treated with MTT for 1 hour at 37°C and the formed formazan crystals were dissolved in DMSO. The extinction was measured spectrophotometrically at λ = 580 nm. The level of reduced glutathione (GSH) was measured using Elmman reagent (MERCK, Germany), which forms colored complexes with SH group at pH 8 with maximum absorbance at 412 nm (Robyt et al., 1971). The resulting absorbance increase was measured spectrophotometrically using SPECTRO UV-VIS AUTO PC Scanning Spectrophotometer (LaboMed, Inc., Los Angeles, CA, USA).

Model of 6-hydroxy dopamine-induced neurotoxicity in isolated rat synaptosomes

6-Hydroxydopamine (6-OHDA) oxidation generates para-quinone and H_2O_2, superoxide and hydroxyl radicals which makes it an appropriate method for modeling the neurotoxicity and the neurodegeneration (Stokes et al., 1999). The rat brain synaptosomes were incubated with the compounds 3–8 (10 μM) for 30 minutes. Thereafter the samples were treated with 6-hydroxydopamnine (150 mM, 1 hour) for induction the neurotoxicity.

Density functional theory calculations

The molecular structure and reaction enthalpies were studied using density functional theory (DFT) calculations. Becke 3-parameter hybrid exchange functional combined with the Lee-Yang-Parr correlation functional (B3LYP) (Becke et al., 1988) with 6-311++G(d,p) basis set were employed in all computations carried out by Gaussian 09 software (Gaussian Inc, Wallingford, CT, USA). The geometry optimization was achieved without any symmetry restrictions. For all structures vibrational frequency analysis was performed and no imaginary frequencies were found. Bond dissociation enthalpy (BDE), proton affinity (PA) and ionization potential (IP) were calculated at 298 K based on the equations reported in the literature (Velkov et al., 2019). The reaction enthalpies in benzene and water were obtained with the Integral Equation Formalism Polarizable Continuum Model (IEF-PCM) (Tomasi et al., 1999).

Molecular docking analysis

The ligand-protein interactions between the tested ligands and the protein molecule MAO-B were studied by molecular docking using Molecular Operating Environment software (MOE Software package 2016, Chemical Computing Group, Montreal, QC, Canada). Protein Data Bank structure was checked, several structural improperties were corrected and non-protein species and water molecules were removed. The missing protons were added according to protonation state of

residues at pH 7.4. Deposited X-ray diffraction structure was in a complex with a ligand, covalently bonded to flavin adenine dinucleotide (FAD) cofactor, therefore we deleted only the ligand by substituting it with a proton. Cavity of the receptor's active site was used without remodeling due to 0.207 nm resolution of X-ray diffraction and cavity formed of residues with low average B values.

A ligand conformation database was constructed according to LowModeMD procedure (Labute et al., 2010) and implemented in the subsequent docking study. Placement of the conformations was carried out using the "Triangle Matcher" method with London dG scoring. "Induced fit" refinement step was followed by scoring with GBVI/WSA dG function (Naïm et al., 2007) as it was implemented in Molecular Operating Environment (MOE) software. Species from poses with the best scoring function was further optimized along with its 0.9 nm proximity with MMFF94 force field.

Oxidative degradation of biologically important molecules

A model system based on the generation of thiobarbituric acid reactive substance products and their subsequent detection at 532 nm was used. As oxidizable substrate was used lecithin (1 mg/mL). A standard agent for induction of oxidative damage – 0.1 mM Fe(II) was applied for the initiation of the oxidative degradation process. All samples were incubated at 37°C for 30 minutes. After the incubation 0.5 mL of 2.8% trichloroacetic acid and 0.5 mL of thiobarbituric acid were added and subsequent second incubation at 100°C was performed. After cooling the tubes at room temperature the ones containing lecithin were centrifuged at 700 × *g* for 20 minutes. The absorbance was measured at 532 nm. Results were presented as "% of molecular damage" determined as percentage of the control sample. Standard reference compounds as Trolox, Melatonin and Quercetin have been tested under the same experimental conditions.

Statistical analysis

Statistical analysis was performed by one-way analysis of variance analysis of variance with Dunnett's *post hoc* test. Differences were accepted to be significant when $P < 0.05$. All statistical analysis was carried out on Graph Pad 6 software (GraphPad Software, Inc., La Jolla, CA, USA).

Results

Chemistry

The synthesis of the N-monoalkylated benzimidazoles was carried out as shown in **Figure 1**. For the preparation of compound 1 was utilized a modification of the phase-transfer catalysis described earlier by Mavrova et al. (2015). The hydrazide 2 and hydrazone 3–8 derivatives were obtained following the same procedures as described in our previous studies (Anastassova et al., 2018a, b) The aim was to synthesize arylhydrazones containing residues of various dihydroxy benzaldehydes (3–5), vanillin (6), 2-hydroxy-4-methoxy benzaldehyde (7) and syringaldehyde (8).

In vitro toxicity of the newly synthesized compounds on SH-SY5Y cells

The cell viability was determined by MTT assay as a marker for mitochondrial function. The SH-SY5Y cells were treated with test compounds in nine different concentrations (ranging from 1 to 1000 μM). The IC_{50} values (half maximal inhibitory concentration) of the compounds (calculated after 24 hours of incubation) were in the range of 89.23 to 311.43 μM (**Table 1**). It should be noted that 6 and 7 were the least toxic compounds with estimated IC_{50} values > 250 μM.

Table 1 | ***In vitro*** **cytotoxicity of the new benzimidazole derivatives (IC_{50} values) on SH-SY5Y cells**

Compound	IC_{50} (μM)	95% Confidence intervals
3	93.65	89.23–111.42
4	89.23	78.32–99.43
5	105.23	92.93–112.43
6	256.12	245.21–262.19
7	311.43	302.01–313.24
8	227.69	212.05–235.45
Melatonin	> 500	
Rasagiline hydrochloride	> 500	

Protective effects of the benzimidazole arylhydrazones in H_2O_2-induced oxidative stress on SH-SY5Y cells

The toxicity of H_2O_2 was confirmed by the observed significant cell viability loss in neuronal cells (**Figure 2**).

As expected, the pretreatment of SH-SY5Y cells with melatonin and rasagiline showed protective effects against H_2O_2-induced oxidative damage. The preincubation with melatonin (1, 10 and 25 μM) caused cell viability protection by 10% ($P < 0.05$), 30% ($P < 0.001$) and 43%, respectively ($P < 0.001$), compared with H_2O_2-treatment, while rasagiline showed protective effects in concentrations of 10 and 25 μM by 25% and 41%, respectively ($P < 0.001$). The test compounds 3–6 and 8 (1, 10 and 25 μM) did not show protective effects on SH-SY5Y cells, whereas the pretreatment with compound 7 considerably reduced the H_2O_2-induced cell damage, showing statistically significant protection by 18%, 71% and 60%, respectively ($P < 0.001$) compared with H_2O_2-induced cell damage.

The neuroprotective effects of compound 7 were also confirmed by microscopic observations on cell morphology (**Figure 3**). It could be noted that compound 7 possesses higher protective effect compared to melatonin and rasagiline in all of the tested concentrations.

In vitro toxicity of the new benzimidazole arylhydrazones on isolated rat brain synaptosomes

The *in vitro* safety evaluation of the new benzimidazole derivatives on SH-SY5Y cells and rat brain synaptosomes showed good safety profile. Compounds 6 and 7 possess the highest IC_{50} values, 256.12 and 311.43 μM respectively, estimated in SH-SY5Y cells *in vitro*. The lowest toxicity of compounds 6 and 7 was also confirmed in rat brain synaptosomes as evaluated by synaptosomal viability and GSH levels.

The evaluation of the potential neurotoxic effects of the arylhydrazone benzimidazole derivatives was performed on freshly isolated rat brain synaptosomes by assessment of the synaptosomal viability (MTT assay) and the levels of GSH. Rat brain synaptosomes are another useful system for studying neuronal metabolism and toxicity. They constitute the subcellular fraction prepared from brain tissue and contain synaptic vesicles (as a source for neurotransmitters), synaptic plasma membranes, and synaptic junctional complexes (Jhou et al., 2017).

The compounds were tested in concentration 50, 100, and 200 μM. All of the compounds revealed concentration-dependent neurotoxicity on isolated rat brain synaptosomes as the effects were most prominent at concentration 200 μM compared to the control of non-treated synaptosomes ($P < 0.01$) (**Figures 4** and **5**). Nevertheless, at all concentrations, compounds 6 and 7 demonstrated the lowest neurotoxicity (*vs*. untreated control, $P < 0.05$). At the highest concentration (200 μM), compound 3 decreased synaptosomal viability and GSH level respectively with 40% and 45%; compound 4 – with 41% and 50%; compound 5 – with 39% and 45%; compound 6 – with 30% and 25%; compound 7 – with 23% and 20%; compound 8 – with 40% and 50%, compared to the control.

At concentration 100 μM, compound 3 decreased synaptosomal viability and GSH level respectively with 30% and with 25%; compound 4 – with 34% and 20%; compound 5 – 31% and 20%; compound 8 – with 28% and 25%. Compound 6 decreased synaptosomal viability with 19% and compound 7 – with 12%. At this concentration, compounds 6 and 7 did not significantly decrease the level of reduced GSH.

At the lowest concentration of 50 μM, the examined compounds decreased statistically significant only the synaptosomal viability. They did not influence the level of GSH. Compound 3 decreased synaptosomal viability with 19%; compound 4 – with 15%; compound 5 – with 11%; compound 8 – with 16%, compared to the control (**Figures 4** and **5**). At 50 μM, compounds 6 and 7 did not show toxicity on the exam parameters.

Protective effects of the new benzimidazole arylhydrazones in a model of induced neurotoxicity in rat brain synaptosomes

The 6-OHDA (150 μM) decreased the synaptosomal viability and the GSH level with 46% and 55%, respectively, compared to the control of non-treated synaptosomes. In the model of 6-OHDA-induced oxidative stress, compound 7 revealed statistically significant neuroprotective effects ($P < 0.05$, *vs*. 6-OHDA). It preserved the synaptosomal viability with 35% and the GSH level with 55 %, compared to 6-OHDA (**Figure 6**). Moreover, its neuroprotective capability of preserving the synaptosomal viability and the GSH levels was exceeding the one of the reference drug rasagiline and was similar to the one of melatonin.

Inhibitory effects of the benzimidazole arylhydrazones on hMAO-B activity

As DA could act as a neurotoxin and thereby takes part in the pathophysiology of neurodegenerative diseases, including PD, and its metabolism and oxidation is catalyzed by MAO-B producing hydrogen peroxide, reactive oxygen species and quinones (Stokes et al., 1999, 2002), the neuroprotective drugs and inhibitors of MAO-B could improve symptoms of PD by prolonging the half-life of DA and prevent further MAO-B-mediated oxidative damage. This is the reason why by the following experiments we evaluated the potential of the new benzimidazole derivatives (1 μM) to inhibit the activity of hMAO-B. Rasagiline and selegiline were used as reference compounds, because of their high potential to irreversibly inhibit MAO-B, and their established neuroprotective activity.

All compounds showed statistically significant MAO-B inhibitory activity (**Figure 7**). Among them compound 7 showed higher hMAO-B inhibition (by 65%) compared to the other test compounds 3, 4, 5, 6, 8. Interestingly, hMAO-B inhibitory effect of compound 7 was similar to those of the classic MAO-B inhibitors selegiline and rasagiline (used as positive controls), since no statistical significant difference between them was found.

Molecular docking study on the interactions with MAO-B

The possible molecular mechanism of action of the arylhydrazone benzimidazole derivatives was elucidated by a docking study in the model of MAO-B (prepared from the published crystal structure of recombinant human MAO-B (Binda et al., 2004). Careful exploration of the active site cavity affirmed its shallow form, as already mentioned by other authors (Carradori and Silvestry 2015; Iacovino et al. 2018). This narrow shape of the cavity explains well the measured good activity of compound 7. The resultant structures from docking obtained after geometry minimization of poses, shows that the rest of the arylhydrazone benzimidazole derivatives even in their best conformations are not long enough to reach the close proximity of FAD. One reasons for that fact is the high lipophilicity of the MAO-B active site pocket, which does not favour interactions with OH and OMe groups. Therefore OH and OMe groups of the phenyl moiety prefer the proximity of water molecules outside the pocket. The other issue is the narrow shape of the entrance, where bigger groups lead to unfavorable steric interactions. This is clearly seen on **Figure 8A**, depicting the optimized positions of compounds 7 and 8 inside the active site cavity of MAO-B, where 7 is situated deeper compared to 8. Compound 7 has phenolic group situated in the proximity of one of the few polar regions inside the pocket – formed by the phenolic group of Tyr326 (purple region close to o-OH in **Figure 8A**), which leads to its further stabilization inside the pocket. As Tyr326 is one of the four boundary residues between the entrance and active site cavities, its position affects which inhibitors are able to bind MAO-B (Binda et al., 2004).

The arrangement of the four residues, Ile199, Phe168, Leu171 and Tyr326, that form the boundary between the two cavities of the enzyme active site, the entrance and the substrate one is clearly visible in **Figure 8B**. Cys172, the well-known (Reis et al. 2018) participant in the interaction between the active site and the MAO-B inhibitors, forms hydrogen bonds with polar parts of the arylhydrazone benzimidazole derivatives studied by us.

Oxidative degradation of lecithin

The ability of the studied compounds to reduce the ferrous iron induced oxidative molecular damage was tested *in vitro* in a lecithin containing model system. All compounds denoted capability to diminish the measured absorbance value at 532 nm compared to the control samples. The extent of molecular damage calculated from these data was lower compared to the controls where maximal oxidative degradation is expected under the described conditions. The observed extent of molecular damage in the presence of melatonin was more than 70% whereas for Trolox and Quercetin around 25%. Several compounds decreased the absorbance values during the experiment to a similar extent – 4, 6, 7 and 8. The determined in the system parameters were respectively – 64.43%, 63.70%, 63.31% and 65.13%. The lowest extent of molecular damage – 47.52% and 38.88%, respectively, was observed in the presence of compounds 5 and 3.

DFT of the most probable mechanisms of antioxidant action

In order to support the assignments of the significant neuroprotective and antioxidant pharmacological activities, the radical-scavenging mechanisms of the most promising compound 7 were evaluated at B3LYP/6-311++G** level of theory. Prior the calculation of BDE, IP and PA, the most stable molecular geometry of 7 was determined by B3LYP/6-311++G** optimization of several probable conformations. As a result, it was found that the benzimidazole fragment is flat and forms approx. 90° angle to those of the arylhydrazone chain. The amide group and the azomethine bond are stabilized in trans configurations. Two major isomers may exist differing by the arrangement around the N-N bond: s-cis or s-trans. However, the s-trans isomer strongly prevails as the energy difference between them is 10.8 kJ•mol^{-1}. The molecular geometry is stabilized by the formation of an intramolecular hydrogen bond between the o-hydroxy group and the azomethine nitrogen atom.

The BDE, IP and PA were evaluated for the more stable s-trans isomer. Benzene and gas phase were accounted in the calculations as nonpolar phases, while water – as polar phase. Hydrogen atom can be abstracted from two possible sites: the amide group, i.e. the N-H bond (site 1, **Figure 9**) and the o-hydroxyl group (site 2, **Figure 10**). The BDE values for the amide N-H group in nonpolar medium: 342 kJ•mol^{-1} (gas phase) and 352 kJ•mol^{-1} (benzene), show that it can more easily transfer a hydrogen atom compared to the o-hydroxyl group: 390 kJ•mol^{-1} (gas phase) and 388 kJ•mol^{-1} (benzene).

In polar medium, i.e. water, the corresponding values of BDE 353 kJ•mol^{-1} (N-H bond, site 1) and ionization potential 325 kJ•mol^{-1} are much higher than the proton affinity 120 kJ•mol^{-1}. Therefore, the sequential proton loss electron transfer (SPLET) mechanism is the preferred one in water.

Discussion

Neuroprotective therapy is aimed at modifying the etiopathogenesis and therefore slowing down the progression of the neurodegenerative disorder. In both idiopathic and genetic cases of PD, oxidative stress is thought to be the common underlying mechanism leading to cellular dysfunction and demise. Increased levels of oxidized lipids (Evans et al., 2017), proteins and DNA, and decreased levels of reduced GSH (Zeevalk et al., 2008) were exhibited in the substantia nigra of PD patients. Because of the presence of reactive oxygen species-generating enzymes such as tyrosine hydroxylase and monoamine oxidase, the DAergic neurons are particularly prone to oxidative stress. In addition, the nigral DAergic neurons contain iron, which catalyzes the Fenton reaction, in which superoxide radicals and hydrogen peroxide can contribute to further oxidative stress (Collin, 2019). Moreover, hydrogen peroxide is generated during DA metabolism by monoamine oxidase which would normally be inactivated by GSH in a reaction catalyzed by glutathione peroxidase. However, if the GSH system is impaired or deficient, H_2O_2 might be converted in the presence of transition metal ions by the iron-mediated Fenton reaction to form highly reactive •OH, so initiating lipid peroxidation and cell death. Therefore the antioxidant activities and neuroprotective effects of the newly synthesized benzimidazole derivatives were evaluated in H_2O_2-induced oxidative stress on SH-SY5Y cells and in a model of 6-OHDA-induced neurotoxicity in rat brain synaptosomes. SH-SY5Y cells possess morphological and biochemical characteristics of human neurons and represent a suitable *in vitro* model for studying the mechanisms of damage and neuroprotection (Agholme et al., 2010; Xicoy et al., 2017). The results from the first model study of H_2O_2-induced oxidative stress on SH-SY5Y cells pointed out that compound 7 possesses a highly promising neuroprotective and antioxidant activity. These effects were even more pronounced than the effects of the referent melatonin and rasagiline. The catecholaminergic neurotoxin 6-OHDA generates hydrogen peroxide and thus induces oxidative stress and damage of the biogenic amine uptake systems (Heikiila et al., 1971). Having in mind that H_2O_2 is generated during the MAO-B enzymatic activity and it plays role in the neurodegenerative process, the 6-OHDA-induced neurotoxicity is an appropriate model for studying the mechanisms of neurotoxicity and neuroprotection. Therefore, the ability of the newly synthetized benzimidazole derivatives to reduce the 6-OHDA-induced oxidative stress was evaluated in rat brain synaptosomes. In the model of 6-OHDA-induced neurotoxicity in rat brain synaptosomes, compound 7 once again revealed significant neuroprotective effects as well by preserving the synaptosomal viability with 35 % and GSH level – with 55 %, compared to 6-OHDA.

All of the new tested N-alkylated benzimidazole arylhydrazones were able of inhibiting hMAO-B activity. Impressively, here once again compound 7 showed the most potent inhibitory effect on hMAO-B, similar to the effects of selegiline and rasagiline that are widely used for PD treatment.

Neuroprotective drugs and the selective monoamine oxidase inhibitors could slow the progression and improve symptoms of PD. Of crucial importance for the better understanding of the pathophysiology and etiology of PD at the molecular and cellular level is finding appropriate molecular targets for neuroprotective and disease-modifying therapy. Therefore, the interactions of the new arylhydrazone benzimidazole derivatives with MAO-B were explored by a docking study.

The MAO-B enzyme features two cavities - substrate and entrance cavity separated by a "gate" amino acid. The one functioning as entrance is highly hydrophobic, whereas the second cavity comprizes the substrate binding site. Crystallographic data of the substrate cavity point to the fact that the amino acid side chains that form the internal pocket/chamber, are very hydrophobic and therefore favor the interaction with an amine moiety. One of the pharmacophores we have selected is the hydrazone group since it is a common structural unit in substrates and inhibitors of MAO enzymes, recognized as crucial for the orientation of the ligand and effective interactions in the active site of the enzyme. The docking study results showed that the potent inhibitory effect of 7 is connected to its appropriate molecular structure enabling the ligand to enter deeper in the narrow and highly lipophylic active site pocket of the hMAO-B and to have a favorable interaction with the key amino acid residues Tyr326 and Cys172.

Much scientific evidence concerning the pathophysiological mechanism of PD points out the implication of iron dysregulation and dyshomeostasis. The increased probability of oxidative damage associated with the elevated oxygen consumption, increased levels of polyunsaturated fatty acids, non-regenerative nature of neurons in combination with a limited application of strong iron chelators that may interfere with the essential for the living organisms iron metabolism, establish as crucial the possibility of new neurodegenerative drug candidates to modulate iron toxicity, especially in the case of a disease associated with regional redox-active metal accumulation, such as PD. All tested compounds influenced the ferrous iron induced oxidative molecular damage. The extent of the effect depends on the structure of the tested hydrazone derivatives. The observed modulation effect was in the same concentration range like the protection effects exerted by the used reference compounds. All investigated compounds denoted protection effect, stronger than the one of melatonin, but lower effectiveness than Trolox and Quercetin. An equivalent effectiveness has been observed among the derivatives containing residues of vanillin and syringaldehyde (6 and 8), methoxy and hydroxy-substituted compound 7 and compound 4 bearing 2,4-dihydroxyl group. These results suggest the substituents cause a similar effect in the model system. The two dihydroxy bearing compounds 3 and 5 having in common a hydroxy group in third position, showed a higher extent of inhibition of iron induced lipid peroxidation of lecithin. On the basis of the data obtained from the spectrophotometric systems for ferrous iron induced oxidative molecular damage, we can conclude that compound 3 – the 2,3 dihydroxy derivative demonstrated the best protection properties.

The radical-scavenging activity of the suggested hydrazones can take place through several mechanisms: HAT (hydrogen atom transfer), SET-PT (single electron transfer-proton transfer) and SPLET. According to the DFT calculations, the preferred mechanism for compound 7 in nonpolar phase is the donation of hydrogen atom from the N-H bond, respectively site 1 (**Figure 10**). The lower activity of the hydroxyl group is due to the intramolecular hydrogen bonding that stabilizes the molecular structure, but hampers the bond dissociation. The diminishing effect of hydrogen bonding on the antioxidant activity has been ascertained by kinetic studies on several phenolic compounds (Amorati et al., 2017). The calculations demonstrated that the most promising hydrazone 7 could exert protective effect in decreasing the harmful effects of the lipid peroxidation by scavenging the LO• and CH_3O• radicals, and prevent the triggered by HOO• radicals lipid peroxidation. In polar medium, i.e. water, proton transfer from the amide group has lower energy requirements than the abstraction of hydrogen atom or electron transfer. Hence the SPLET mechanism is expected to be the main mechanism of radical

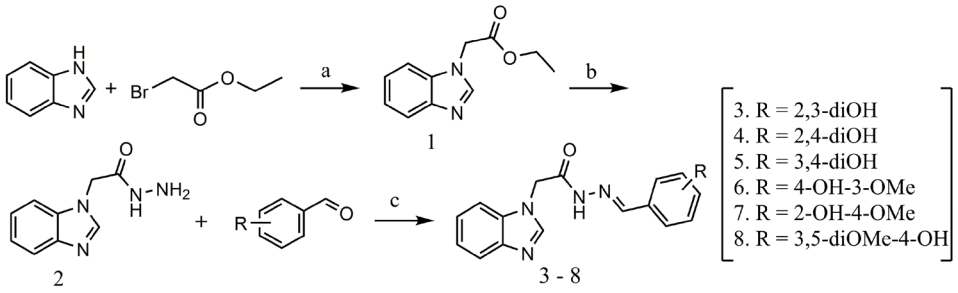

Figure 1 | Synthesis of the studied compounds.
Reagents and conditions: (a) dimethylformamide, K_2CO_3, tetrabutylammonium hydrogen sulfate (TBAHS); (b) hydrazine hydrate, ethanol, reflux; (c) substituted benzaldehyde, absolute ethanol, reflux.

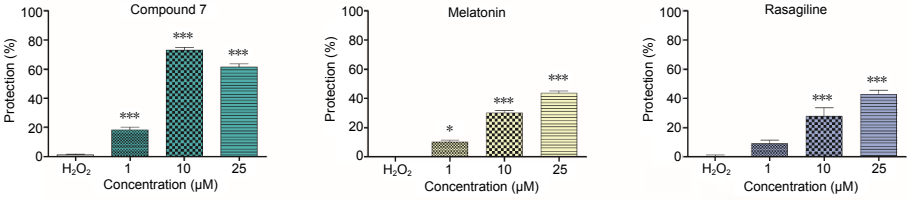

Figure 2 | Protective effects of compound 7, melatonin, and rasagiline in a model of H_2O_2-induced oxidative damage in human neuroblastoma SH-SY5Y cells.
Data are presented as means from three independent experiments ± SD (n = 8). *P < 0.05, ***P < 0.001, *vs.* H_2O_2 group (one-way analysis of variance with Dunnet's *post hoc* test).

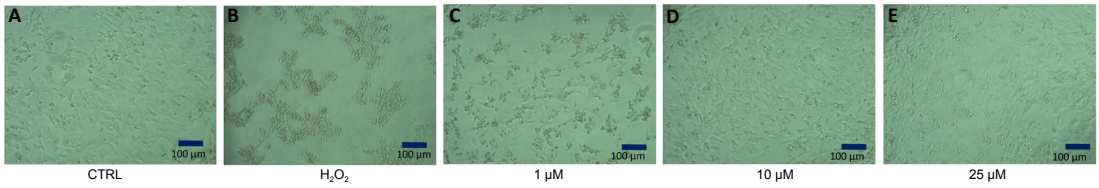

Figure 3 | Microphotographs of human neuroblastoma SH-SY5Y cells.
The microphotographs were taken with phase-contrast microscope OPTIKA (OPTIKA®Italy, Bergamo, Italy). (A) Negative control, untreated cells. (B) Positive control, cells treated with H_2O_2; (C) Cells treated with compound 7 (1 μM) for 60 minutes before H_2O_2 exposure. (D) Cells treated with compound 7 (10 μM) for 60 minutes before H_2O_2 exposure. (E) Cells treated with compound 7 (25 μM) for 60 minutes before H_2O_2 exposure.

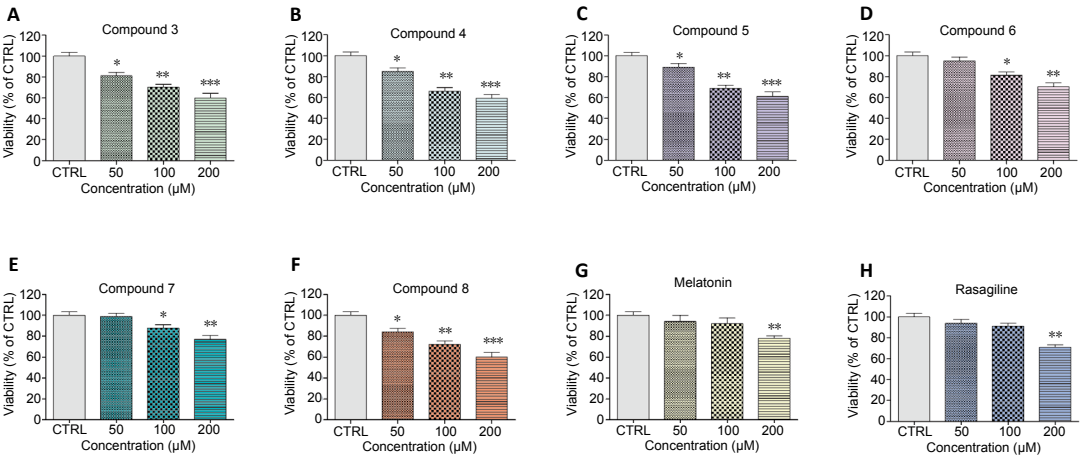

Figure 4 | Effect of the new benzimidazole derivatives on synaptosomal viability.
Synaptosomal viability was assessed after treatment with various concentrations of the new benzimidazole arylhydrazones (50, 100 and 200 μM): compound 3 (A), compound 4 (B), compound 5 (C), compound 6 (D), compound 7 (E), compound 8 (F) and after treatment with the reference compounds melatonin (G) and rasagiline (H) at the same concentrations. Data are presented as means from five independent experiments ± SD (n = 3). *P < 0.05, **P < 0.01, ***P < 0.001, *vs.* control group (one-way analysis of variance with Dunnet's *post hoc* test).

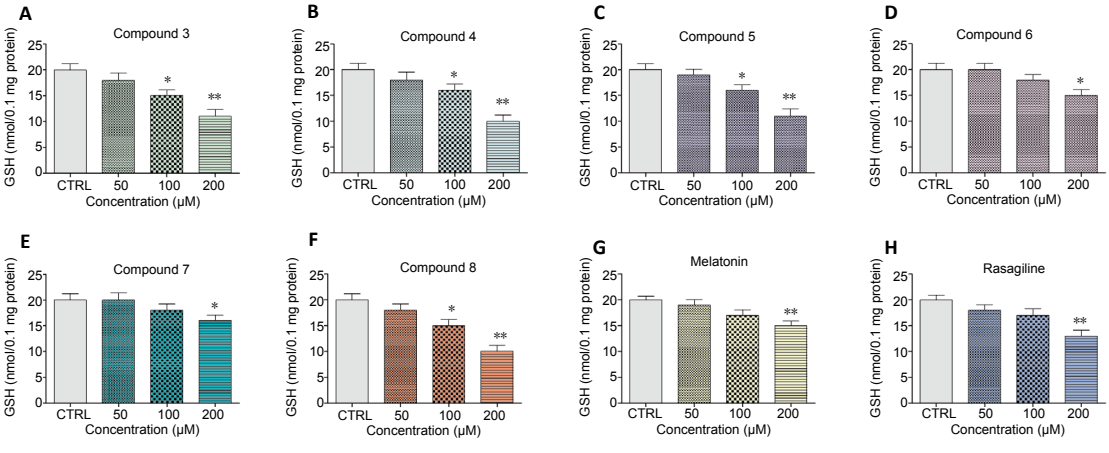

Figure 5 | Effect of the new benzimidazole derivatives on GSH level in rat brain synaptosomes.
The GSH levels were assessed after treatment with various concentrations of the new benzimidazole arylhydrazones (50, 100 and 200 μM): compound 3 (A), compound 4 (B), compound 5 (C), compound 6 (D), compound 7 (E), compound 8 (F) and after treatment with the reference compounds melatonin (G) and rasagiline (H) at the same concentrations. Data are presented as means from five independent experiments ± SD (n = 3). *P < 0.05, **P < 0.01, ***P < 0.001, *vs.* control group (one-way analysis of variance with Dunnet's *post hoc* test).

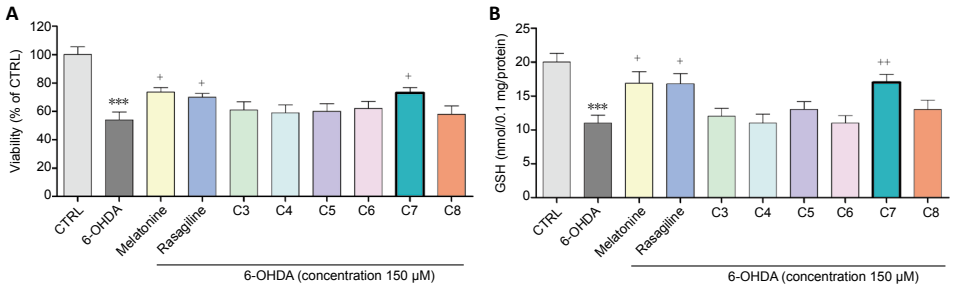

Figure 6 | Effect of the new benzimidazole on synaptosomal viability and GSH levels in a model of 6-OHDA induced oxidative stress.
(A) Effect of the tested benzimidazole aryhydrazones C3–C8 (10 µM) on the synaptosomal viability in a model of 6-OHDA (150 µM) induced oxidative stress compared to the referent compounds rasagiline and melatonine. (B) Effect of the tested benzimidazole aryhydrazones C3–C8 (10 µM) on the GSH levels in a model of 6-OHDA (150 µM) induced oxidative stress. Data are represented as means from five independent experiments ± SD (n = 3). ***P < 0.001, *vs*. untreated control (CTRL) group; +P < 0.05, ++P < 0.01, *vs*. 6-OHDA (one-way analysis of variance with Dunnet's *post hoc* test). 6-OHDA: 6-Hydroxydopamine; C3–C8: compounds 3–8; GSH: glutathione.

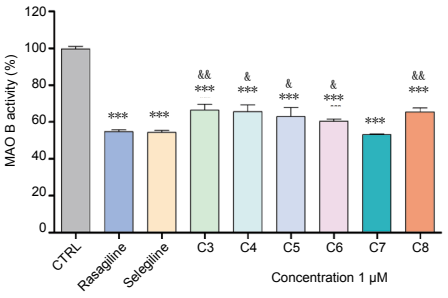

Figure 7 | *In vitro* inhibitor activity of the new benzimidazole derivatives on human recombinant MAO-B enzyme.
Data are presented as means from three independent experiments ± SD (n = 8). Groups were compared by one-way analysis of variance with Dunnet's *post hoc* test. ***P < 0.001, *vs*. control group; &P < 0.05, &&P < 0.01, vs. Compound 7. MAO-B: monoamine oxidase-B. C3–C8: Compounds 3–8.

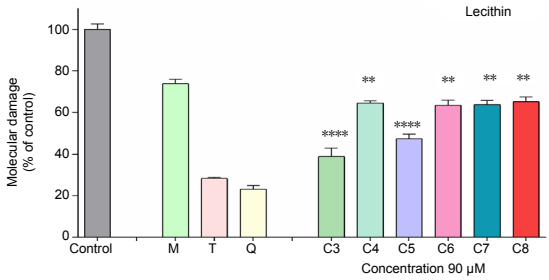

Figure 9 | Effect of the tested hydrazone derivatives on the in vitro Fe(II) induced oxidative degradation in lecithin containing model system (1 mg/mL) with compounds concentration (90 µM).
Melatonin (M), Trolox (T), and Quercetin (Q) at the same concentration have been used as reference compounds. Data are presented as means from three independent experiments ± SD (n = 3). Groups were compared by one-way analysis of variance with Dunnet's *post hoc* test; **P < 0.01, ****P < 0.0001, *vs*. Melatonin group. C3–C8: Compounds 3–8.

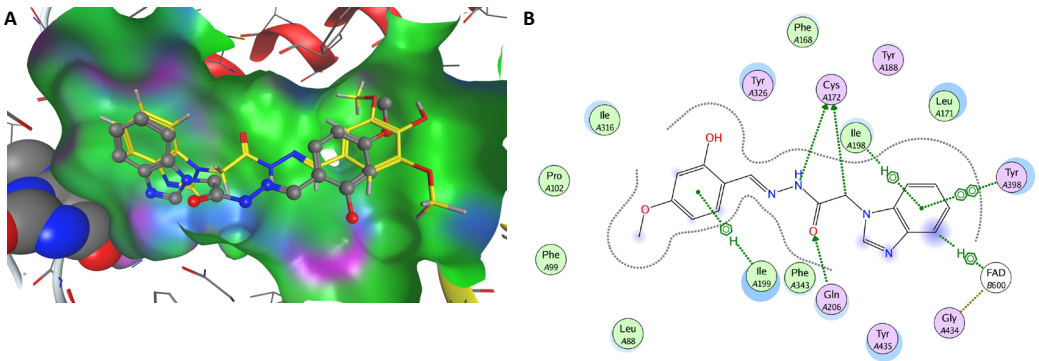

Figure 8 | The most favorable interacting derivative 7 inside the MAO-B pocket.
(A) Derivative 7 (represented with gray carbons) compared to 8 (represented with yellow carbons) derivative inside the MAO-B active site pocket. The distant side of the pocket is represented from van der Waals (vdW) radii; lipophilic parts are depicted in green; polar are in pink and blue color. The closest part of flavine cofactor is seen on the left, with atoms represented as van der Waals spheres. (B) Schematic depiction of the close proximity to the most active derivative 7 inside the MAO-B pocket. MAO-B: Monoamine oxidase-B.

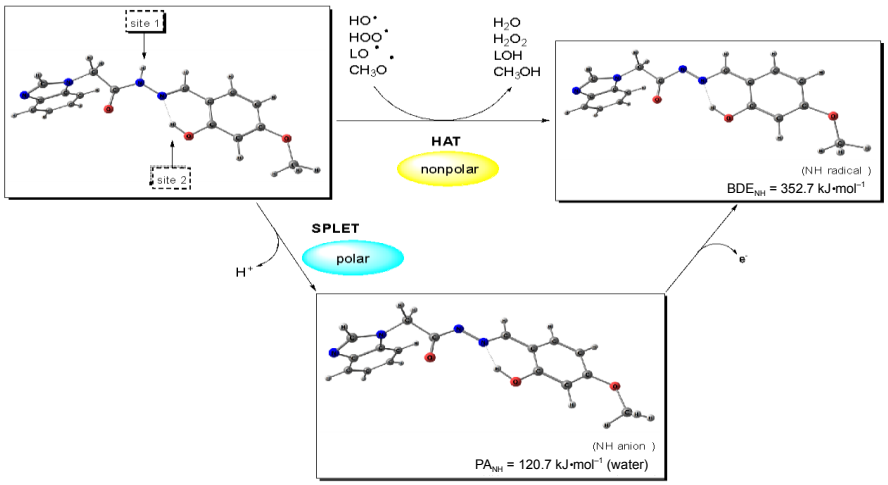

Figure 10 | Predicted mechanisms of radical scavenging by compound 7 in nonpolar (benzene) and polar phase (water).
For an effective antioxidant action and inhibition of the lipid peroxidation, the radical corresponding to the antioxidant agent should have significant stability and be less reactive regarding the attacked radicals. As a consequence the calculated BDE of hydrazone 7 should be lower than the BDE values of the free radicals. For the accurate estimation of the RSA, it is necessary to compare the BDE of compound 7 to the calculated BDE values of free radicals in benzene: 339 kJ•mol^{-1} (model LOO•, (Z)-4-hydroperoxyhex-2-enyl radical), 344 kJ•mol^{-1} (CH_3OO•), 353 kJ•mol^{-1} (HOO•), 424 kJ•mol^{-1} (model LO•, (Z)-4-hydroxyhex-2-enyl radical), 418 kJ•mol^{-1} (CH_3O•), 489 kJ•mol^{-1} (HO•). The comparison showed that hydrazone 7 has higher BDE than LOO• and CH_3OO•, but lower BDE than HOO•, LO•, CH_3O•, and HO•.

scavenging in water and in polar organic solvents (**Figure 10**).

Conclusion

The safety profile of the newly synthesized compounds is an important part of their characterization. The *in vitro* safety evaluation of the new benzimidazole derivatives on SH-SY5Y cells and rat brain synaptosomes showed good safety profile. Moreover, the isomer compounds 6 and 7 containing one hydroxy and one methoxy group possess the highest IC_{50} values, 256.12 and 311.43 μM estimated *in vitro* on SH-SY5Y cells. The lowest toxicity of compounds 6 and 7 was also confirmed in the rat brain synaptosomes as evaluated by synaptosomal viability and GSH levels.

The antioxidant activities and neuroprotective effects of the newly synthesized benzimidazole derivatives were evaluated in H_2O_2-induced oxidative stress on SH-SY5Y cells and in a model of 6-OHDA-induced neurotoxicity in rat brain synaptosomes. The results showed that 7 demonstrated significant neuroprotective activity. These effects were even more pronounced than the effects of the referent compounds melatonin and rasagiline.

All the new tested compounds significantly inhibited hMAO-B activity. Interestingly, once again compound 7 showed the most potent inhibitory effect on hMAO-B, similar to the one of the referent PD drugs selegiline and rasagiline. According to the performed molecular docking studies, compound 7 is able to interact in the most favorable way with the highly lipophilic and narrow active pocket of the MAO-B enzyme, that does not favor steric interactions with bigger functional groups.

The studied compounds also demonstrated the ability to reduce the ferrous iron induced oxidative molecular damage of lecithin used as a lipid peroxidation model. However, the observed relative activity did not follow all the trends established by the *in vitro* models in SH-SY5Y cells and rat brain synaptosomes, therefore indicating the crucial role of the MAO-B inhibitory activity of compound 7 for its neuroprotective effects.

In conclusion, the new benzimidazole derivative 7 possesses good safety profile, stronger neuroprotective properties than melatonin and rasagiline and similar MAO-B inhibitory effect as rasagiline and selegiline. Additionally, it is capable of protecting from Fe-incuded lipid peroxidation, and thereby might protect the cell membranes of oxidative stress. Therefore, the present study outlines a perspective leading structure, bearing the potential for a new anti-PD drug that will be subjected to further pharmacological testing.

Author contributions: *Study concept and design: NA and DY; synthesis, characterization and interpretation: NA, AK, NL; cell viability assay, phase-contrast micrographs, statistical analysis: DA; oxidative stress in cell cultures, evaluation of hMAOB activity: VT, synaptosomal viability assay and neuroprotective effect: MKB; docking studies: MR and NT; oxidative degradation of lecithin: NHA; DFT methods: MA and DY. All authors contributed for the manuscript writing and approved the final version of the paper.*
Conflicts of interest: *The authors declare that they have no competing interests.*
Financial support: *This work was supported by the National Science Fund of Bulgaria (Young scientists project contract КП-06-М29/4; to NA, MA, NHA, and DA).*
Institutional review board statement: *All performed procedures were approved by the Institutional Animal Care Committee of the Medical University of Sofia (Bulgarian Agency for Food Safety with Permission № 190, approved on February 6, 2020).*

Data sharing statement: *Datasets analyzed during the current study are available from the corresponding author on reasonable request.*
Plagiarism check: *Checked twice by iThenticate.*
Peer review: *Externally peer reviewed.*

References

Agholme L, Lindström T, Kågedal K, Marcusson J, Hallbeck M (2010) An in vitro model for neuroscience: differentiation of SH-SY5Y cells into cells with morphological and biochemical characteristics of mature neurons. J Alzheimers Dis 20:1069-1082.

Amorati R, Baschieri A, Cowde A, Valgimigli L (2017) The antioxidant activity of quercetin in water solution. Biomimetics 2: 9-21

Anastassova N, Mavrova A, Yancheva D, Kondeva-Burdina M, Tzankova V, Stoyanov S, Shivachev B, Nikolova R (2018a) Hepatotoxicity and antioxidant activity of some new N,N'-disubstituted benzimidazole-2-thiones, radical scavenging mechanism and structure-activity relationship. Arab J Chem 11:353-369.

Anastassova N, Yancheva D, Mavrova A, Kondeva-Burdina M, Tzankova V, Hristova-Avakumova N, Hadjimitova V (2018b) Design, synthesis, antioxidant properties and mechanism of action of new N,N'-disubstituted benzimidazole-2-thione hydrazine derivatives. J Mol Struct 1165:162-176.

Anastassova NO, Yancheva DY, Argirova MA, Hadjimitova VV, Hristova-Avakumova NG (2019) In vitro assessment of the antioxidant activity of new benzimidazole-2-thione hydrazone derivatives and DFT study of their mechanism of action. Bulgarian Chem Comm 51:186-192.

Anastassova N, Yancheva D, Hristova-Avakumova N, Hadjimtova V, Traykov T, Aluani D, Tzankova V, Kondeva-Burdina M (2020) New benzimidazole-aldehyde hybrids as neuroprotectors with hypochlorite and superoxide radical-scavenging activity. Pharmacol Rep 72:846-856.

Bautista-Aguilera OM, Esteban G, Bolea I, Nikolic K, Agbaba D, Moraleda I, Iriepa I, Samadi A, Soriano E, Unzeta M, Marco-Contelles J (2014) Design, synthesis, pharmacological evaluation, QSAR analysis, molecular modeling and ADMET of novel donepezil-indolyl hybrids as multipotent cholinesterase/monoamine oxidase inhibitors for the potential treatment of Alzheimer's disease. Eur J Med 75:82-95.

Becke A (1993) Density-functional thermochemistry. III. The role of exact exchange. J Chem Phys 98:5648-5652.

Binda C, Newton-Vinson P, Hubálek F, Edmondson DE, Mattevi A (2002) Structure of human monoamine oxidase B, a drug target for the treatment of neurological disorders. Nat Struct Biol 9:22-26.

Carradori S, Ortuso F, Petzer A, Bagetta D, De Monte C, Secci D, De Vita D, Guglielmi P, Zengin G, Aktumsek A, Alcaro S, P Petzer J (2018) Design, synthesis and biochemical evaluation of novel multi-target inhibitors as potential anti-Parkinson agents. Eur J Med Chem 143:1543-1552.

Carradori S, Silvestri R (2015) New frontiers in selective human MAO-B inhibitors. J Med Chem 58:6717-6732.

Collin F (2019) Chemical basis of reactive oxygen species reactivity and involvement in neurodegenerative diseases. Int J Mol Sci 20:2407-2423.

Dezsi L, Vecsei L (2017). Monoamine oxidase B inhibitors in Parkinson's disease. CNS Neurol Disord Drug Targets 16:425-439.

Evans T, Kok WL, Cowan K, Hefford M, Anichtchik O (2017) Accumulation of beta-synuclein in cortical neurons is associated with autophagy attenuation in the brains of dementia with Lewy body patients. Brain Res 1681:1-13.

Finberg JPM, Rabey JM (2016) Inhibitors of MAO-A and MAO-B in psychiatry and neurology. Front Pharmacol 7:340.

Freitas ME, Ruiz-Lopez M, Fox SH (2016) Novel levodopa formulations for Parkinson's disease. CNS Drugs 30:1079-1095.

Goggi J, Theofilopoulos S, Riaz SS, Jauniaux E, Gerald MS, Bradford HF (2000) The neuronal survival effects of rasagiline and deprenyl on fetal human and rat ventral mesencephalic neurones in culture. Neuroreport 11:3937-3941.

Halliwell B (1992) Reactive oxygen species and the central nervous system. J Neurochem 59:1609-1623.

Hattori N, Takeda A, Takeda S, Nishimura A, Nakaya R, Mochizuki H, Nagai M, Takahashi R (2019) Long-term safety and efficacy of adjunctive rasagiline in levodopa-treated Japanese patients with Parkinson's disease. J Neural Transm 3:289-297.

Heikiila R, Cohen G (1971) Inhibition of biogenic amine uptake by hydrogen peroxide: a mechanism for toxic effects of 6-hydroxydopamine. Science 172:1257-1258.

Hirata Y, Yamada C, Ito Y, Yamamoto S, Nagase H, Oh-hashi K, Kiuchi K, Suzuki H, Sawada M, Furuta K (2018) Novel oxindole derivatives prevent oxidative stress-induced cell death in mouse hippocampal HT22 cells. Neuropharmacology 135:242-252.

Iacovino LG, Magnani F, Binda C (2018) The structure of monoamine oxidases: past, present, and future. J Neural Transm 11:1567-1579.

Inaba-Hasegawa K, Shamoto-Nagai M, Maruyama W, Naoi M (2017) Type B and A monoamine oxidase and their inhibitors regulate the gene expression of Bcl-2 and neurotrophic factors in human glioblastoma U118MG cells: different signal pathways for neuroprotection by selegiline and rasagiline. J Neural Transm 9:1055-1066.

Jhou JF, Tai HC (2017) The study of postmortem human synaptosomes for understanding Alzheimer's disease and other neurological disorders: a review. Neurol Ther 6:57-68.

Labute P (2010) LowModeMD--implicit low-mode velocity filtering applied to conformational search of macrocycles and protein loops. J Chem Inf Model 50:792-800.

Lee C, Yang W, Parr GR (1988) Development of the Colle-Salvetti correlation-energy formula into a functional of the electron density. Phys Rev B 37:785-789.

Lowry OH, Rosebrough NJ, Farr AL, Randall RJ (1951) Protein measurement with the Folin phenol reagent. J Biol Chem 193:265-275.

Matos MJ, Ibatá DMH, Uriarte E, Viña D (2020) Coumarin-rasagiline hybrids as potent and selective hMAO-B inhibitors, antioxidants and neuroprotective agents. Chem Med Chem 15:532-538.

Mavrova A, Yancheva D, Anastassova N, Anichina K, Zvezdanovic J, Djordjevic A, Markovic D, Smelcerovic A (2015) Synthesis, electronic properties, antioxidant and antibacterial activity of some new benzimidazoles. Bioorg Med Chem 23:6317-6326.

Mossmann T (1983) Rapid colorimetric assay for cellular growth and survival: application to proliferation and cytotoxicity assays. J Immunol Methods 65:55-36.

Mungarro-Menchaca X, Ferrera P, Morán J, Arias C (2002) β-Amyloid peptide induces ultrastructural changes in synaptosomes and potentiates mitochondrial dysfunction in the presence of ryanodine. J Neurosci Res 68:89-96.

Naïm M, Bhat S, Rankin KN, Dennis S, Chowdhury SF, Siddiqi I, Drabik P, Sulea T, Bayly CI, Jakalian A, Purisima EO (2007) Solvated interaction energy (SIE) for scoring protein-ligand binding affinities. 1. Exploring the parameter space. J Chem Inf Model 47:122-133.

Reis J, Manzella N, Cagide F, Mialet-Perez J, Uriarte E, Parini A, Borges F, Binda C (2018) Tight-binding inhibition of human monoamine oxidase B by chromone analogs: a kinetic, crystallographic, and biological analysis. J Med Chem 61:4203-4212.

Robyt JF, Ackerman RJ, Chittenden CG (1971) Reaction of protein disulfide groups with Ellman's reagent: A case study of the number of sulfhydryl and disulfide groups in Aspergillus oryzae alpha-amylase, papain, and lysozyme. Arch Biochem Biophys 147:262-9.

Secci D, Carradori S, Petzer A, Guglielmi P, D'Ascenzio M, Chimenti P, Bagetta D, Alcaro S, Zengin G, Petzer JP, Ortuso F (2019) 4-(3-Nitrophenyl)thiazol-2-ylhydrazone derivatives as antioxidants and selective hMAO-B inhibitors: synthesis, biological activity and computational analysis. J Enz Inh Med Chem 34:597-612.

Stokes AH, Freeman WM, Mitchell SG, Burnette TA, Hellmann GM, Vrana KE (2002) Induction of GADD45 and GADD153 in neuroblastoma cells by dopamine-induced toxicity. Neurotoxicology 23:675-684.

Stokes AH, Hastings TG, Vrana KE (1999) Cytotoxic and genotoxic potential of dopamine. J Neurosci Res 55:659-665.

Taupin P, Zini S, Cesselin F, Ben-Ari Y, Roisin MP (1994) Subcellular fractionation on Percoll gradient of mossy fiber synaptosomes: morphological and biochemical characterization in control and degranulated rat hippocampus. J Neurochem 62:1586-1595.

Tomasi J, Mennucci B, Cancès E (1999) The IEF version of the PCM solvation method: an overview of a new method addressed to study molecular solutes at the QM ab initio level. J Mol Struct 464:211-226.

Uddin MS, Kabir MT, Rahman MH, Alim MA, Rahman MM, Khatkar A, Al Mamun A, Rauf A, Mathew B, Ashraf GM (2020) Exploring the multifunctional neuroprotective promise of rasagiline derivatives for multi-dysfunctional Alzheimer's disease. Curr Pharm Des 37:4690-4698.

Watson N, Diamandis T, Gonzales-Portillo C, Reyes S, Borlongan CV (2016) Melatonin as an antioxidant for stroke neuroprotection. Cell Transplant 25:883-891.

Weinreb O, Amit T, Bar-Am O, Youdim MBH (2010) Rasagiline: A novel anti-Parkinsonian monoamine oxidase-B inhibitor with neuroprotective activity. Prog Neurobiol 92:330-344.

Wingo TS, Rosen A, Cutler DJ, Lah JJ, Levey AI (2012) Paraoxonase-1 polymorphisms in Alzheimer's disease, Parkinson's disease, and AD-PD spectrum diseases. Neurobiol Aging 33:204, e213-215.

Wu Y, Shamoto-Nagai M, Maruyama W, Osawa T, Naoi M (2017) Phytochemicals prevent mitochondrial membrane permeabilization and protect SH-SY5Y cells against apoptosis induced by PK11195, a ligand for outer membrane translocator protein. J Neural Transm 1:89-98.

Velkov Z, Traykov M, Trenchev I, Saso L, Tadjer A (2019) Topology-dependent dissociation mode of the O–H bond in monohydroxycoumarins. J Phys Chem A 123:5106-5113.

Xicoy H, Wieringa B, Martens GJM (2017) The SH-SY5Y cell line in Parkinson's disease research: a systematic review. Mol Neurodegener 12:10-20.

Zeevalk GD, Razmpour R, Bernard LP (2008) Glutathione and Parkinson's disease: is this the elephant in the room? Biomed Pharmacoter 62:236-249.

C-Editors: Zhao M, Li CH; T-Editor: Jia Y